

NP-11-0020
May 23, 2011

10 CFR 52, Subpart A

U.S. Nuclear Regulatory Commission
ATTN: Document Control Desk
Washington, DC 20555-0001

Subject: Exelon Nuclear Texas Holdings, LLC
Victoria County Station Early Site Permit Application
Response to Request for Additional Information Letter No. 07
NRC Docket No. 52-042

Attached are responses to NRC staff questions included in Request for Additional Information (RAI) Letter No. 07, dated April 8, 2011, related to Early Site Permit Application (ESPA), Part 2, Sections 02.04.06, 02.05.02, and 11.02. NRC RAI Letter No. 07 contained twenty (20) Questions. This submittal comprises a partial response to RAI Letter No. 07, and includes responses to the following seven (7) Questions:

02.04.06-2	02.05.02-3(d)
	02.05.02-4
	02.05.02-5
	02.05.02-6(a)
	02.05.02-6(b)
	02.05.02-9

When a change to the ESPA is indicated by a Question response, the change will be incorporated into the next routine revision of the ESPA, planned for no later than March 31, 2012.

Of the remaining thirteen (13) RAIs associated with RAI Letter No. 07, responses to seven (7) Questions were submitted to the NRC in Exelon Letter NP-11-0016, dated May 5, 2011. The response to RAI Question 02.05.02-6c will be provided by June 22, 2011. The response to RAI Questions 02.04.06-3 and 02.05.02-10 will be provided by July 7, 2011. The response to RAI Questions 02.05.02-3a, 02.05.02-3b, and 02.05.02-3c will be provided by August 5, 2011. These response times are consistent with the response times described in NRC RAI Letter No. 07, dated April 8, 2011.

The responses to RAI Questions 02.05.02-3(d) and 02.05.02-5 include electronic data files provided on enclosed CDs. Two copies of the electronic data CDs are enclosed, one CD for submission to the Public Document Room and one CD for NRC staff use.

Regulatory commitments established in this submittal are identified in Attachment 8.

D087
NRD

If any additional information is needed, please contact David J. Distel at (610) 765-5517.

I declare under penalty of perjury that the foregoing is true and correct. Executed on the 23rd day of May, 2011.

Respectfully,



Marilyn C. Kray
Vice President, Nuclear Project Development

Attachments:

1. Question 02.04.06-2
2. Question 02.05.02-3(d)
3. Question 02.05.02-4
4. Question 02.05.02-5
5. Question 02.05.02-6(a)
6. Question 02.05.02-6(b)
7. Question 02.05.02-9
8. Summary of Regulatory Commitments
9. CD-R labeled: RAI 02.05.02-3(d) SOURCE-GEOMETRY.TXT (Two copies)
10. CD-R labeled: RAI 02.05.02-5 RGR-GEOMETRY.TXT (Two copies)

cc: USNRC, Director, Office of New Reactors/NRLPO (w/Attachments)
USNRC, Project Manager, VCS, Division of New Reactor Licensing (w/Attachments)
USNRC Region IV, Regional Administrator (w/Attachments)

RAI 02.04.06-2:**Question:**

To meet the requirements of GDC 2, 10 CFR 52.17, and 10 CFR Part 100, an assessment of the Probable Maximum Tsunami (PMT) for the proposed site should be provided in the application. Section C.1.2.4.6.2 of Regulatory Guide 1.206 (RG 1.206) provides specific guidance with respect to the historical tsunami record, including paleo-tsunami evidence. Provide in the SSAR information regarding geologic evidence of tsunami deposits at the Victoria County site or at nearby regions, such as from borings or other subsurface information collected by the applicant. Cross-reference with Section 2.5 of the SSAR where applicable. Additionally, indicate whether there are geologically conducive locations for the deposition and preservation of tsunami deposits in the vicinity of the Victoria County site. If such paleo-tsunami evidence exists, indicate how they are distinguished from storm wash-over deposits.

Response:

The initial subsurface investigation at VCS included obtaining samples and data from over 150 borings drilled within and around the Power Block area and in the area of the cooling basin. Sixty-five cone penetration tests (CPTs), geophysical logging, and laboratory testing were also performed for the subsurface investigation. A supplemental investigation included drilling an additional 94 borings and performing 12 additional CPTs as well as geophysical logging and laboratory testing. Boring and cross section locations are shown on SSAR Figures 2.5.1-33, 2.5.4-A-1, and -A-4. Cross sections/subsurface profiles showing the unconsolidated deposits of the Beaumont Formation are presented in SSAR Figures 2.5.1-34 and -35; Figures 2.5.4-3, -5, -6, -9 and -10; Figures 2.5.4-14 through -20; and Figures 2.5.4-A-5, -6, -7, and -9 through -11. The Beaumont Formation at the site is an interbedded sequence of sands and clays with occasional gravels that extends from the ground surface to depths of about 600 feet. SSAR Subsection 2.5.1.2.3 describes site stratigraphy. In general, the sands are light gray/brown/yellow, fine to medium grained silty, clayey deposits. Occasional gravel deposits are also present. Based on electric log signatures, grain size analysis, and distribution across the site, these sands are interpreted as distributary channel deposits. The clay units appear to be overbank and flood plain deposits. These interpretations are consistent with the geologic mapping performed at the site (SSAR Figures 2.5.1-4 and -5) and the interpretations by Blum and Aslan (2006) of the Beaumont Formation that are applicable to the broader 25-mile radius site vicinity. Gravel deposits are reported in borings in the cooling basin area and in boring B-2324, which has more than 30 feet (9 meters) of gravel at the top of the boring. Boring B-2324 is located on the flood plain of the Guadalupe River where gravel deposits are expected and mapped on the surface (Unit Qt on Figure 2.5.1-4).

Several criteria have been proposed for characterizing tsunami deposits and differentiating them from storm deposits. Tuttle et al. (2004) compare deposits from the 1929 Grand Banks earthquake-induced tsunami and the 1991 "Halloween" storm. Tuttle et al. (2004) propose that four criteria can be used to distinguish between the tsunami and storm deposits based on sedimentary characteristics, diatom content, biostratigraphic assemblages, and landscape position. These criteria are described in more detail in the proposed revision to SSAR Subsection 2.5.1.2.5 provided below. Morton et al. (2007) attribute the differences between tsunami and storm deposits to differences in the hydrodynamics and sediment-sorting process during transport. However, Shanmugam (2011) refutes the notion that a tsunami event represents a single depositional process and contends that tsunami deposits cannot be

distinguished from storm deposits using sedimentological features without considering historical information as well.

Regardless of the uncertainty in characterizing tsunami deposits and differentiating them from storm deposits, no soil deposits with the characteristics of tsunamigenic or storm surge deposition documented by Tuttle et al. (2004) or summarized by Shanmugam (2011) were encountered at VCS, nor are such deposits described by Blum and Aslan (2006) for the site vicinity. In addition, geologic mapping and subsurface exploration do not indicate the presence of modern or paleo-geographic environments that might have preserved tsunami or storm deposits (future SSAR 2.5.1.2.5 revision).

References

Blum, M. D., and Aslan, A., Signatures of Climate vs. Sea-Level Change within Incised Valley-Fill Successions: Quaternary Examples from the Texas Gulf Coast, *Sedimentary Geology*, v. 190, p. 177-211, 2006.

Morton, R., Gelfenbaum G., and Jaffe, B., "Physical Criteria for Distinguishing Sandy Tsunami and Storm Deposits using Modern Examples." *Sedimentary Features of Tsunami Deposits-Their Origin, Recognition, and Discrimination*, Tappin, D. (ed.), *Sedimentary Geology*, v. 200, no 3-4, (special issue) pp. 184-207, 2007.

Shanmugam, G., "Process-sedimentological challenges in distinguishing paleo-tsunami deposits," *Natural Hazards*, Springer, 2011.

Tuttle, M., Ruffman, A., Anderson, T. Jeter, H., "Distinguishing Tsunami from Storm Deposits in Eastern North America: The 1929 Grand Banks Tsunami versus the 1919 Halloween Storm," *Seismological Research Letters*, v. 75, no. 1, p. 117-131, 2004

Associated ESPA Revisions:

SSAR Subsection 2.4.6.2 will be revised in a future revision to the ESPA, as indicated:

2.4.6.2 Historical Tsunami Record

Records of historical tsunami runup events in the Texas Gulf Coast are obtained from the National Geophysical Data Center (NGDC) tsunami database. The NGDC database contains information on source events and runup elevations for worldwide tsunamis from about 2000 B.C. to the present time (Reference 2.4.6-8). A search of the NGDC tsunami database returned three historical tsunamis that have affected the Texas Gulf Coast as indicated in Table 2.4.6-1.

The first recorded tsunami event occurred on October 24, 1918, and was presumed to be caused by an aftershock of the October 11, 1918, earthquake (moment magnitude scale, $M_w=7.3$) near Puerto Rico (References 2.4.6-8 and 2.4.6-9). The NGDC database did not provide a runup height for this event although it is classified as a definite tsunami event. The second tsunami event in the Texas Gulf Coast region occurred on May 2, 1922, and is related to a small earthquake at the Island of Vieques, Puerto Rico. A tsunami runup height of 0.64 meters (2.1 feet) from a tide-gauge measurement at Galveston, Texas, was reported. However, according to the NGDC database, the slight shock was unlikely to have been the tsunamigenic source. This event is classified as a doubtful tsunami in the NGDC database.

The third reported tsunami event occurred on March 27, 1964, in Alaska Standard Time or March 28, 1964, in Universal Coordinated Time (UCT), and was due to seismic seiche induced by the Great Alaska Earthquake (Reference 2.4.6-6) as discussed in Subsection 2.4.6.1. Although water level oscillations were recorded on several tide stations including Freeport, Texas, no runup height is provided in the NGDC database. However, other data sources indicate that the seiche double amplitudes measured at the Texas Gulf Coast tide stations are in the range of 0.22 to 0.84 feet (0.07 to 0.26 meters) and is 0.66 feet (0.2 meters) at Freeport, Texas (Reference 2.4.6-5).

Other tsunami events affecting the Gulf of Mexico region are mainly from the Caribbean sources (References 2.4.6-9 and 2.4.6-10). However, the Texas Gulf Coast remained mostly unaffected during these tsunamis. An extensive literature search did not reveal any evidence of seismic source-induced paleotsunami deposit in the region.

Looking beyond the historical record, the geologic record investigated by surface and subsurface investigations of the Beaumont Formation indicates the absence of tsunamigenic and/or storm surge deposits at VCS. The initial subsurface investigation at VCS included obtaining samples and data from over 150 borings drilled within and around the Power Block area and in the area of the cooling basin. Sixty-five cone penetration tests (CPTs), geophysical logging, and laboratory testing were also performed for the subsurface investigation. A supplemental investigation included drilling an additional 94 borings and performing 12 additional CPTs as well as geophysical logging and laboratory testing. Boring and cross section locations are shown on SSAR Figures 2.5.1-33, 2.5.4-A-1, and -A-4. Cross sections/subsurface profiles showing the unconsolidated deposits of the Beaumont Formation are presented in SSAR Figures 2.5.1-34 and -35; Figures 2.5.4-3, -5, -6, -9 and -10; Figures 2.5.4-14 through -20; and Figures 2.5.4-A-5, -6, -7, and -9 through -11. In general, the sands are gray/brown/yellow, fine to medium grained silty, clayey deposits. Occasional gravel deposits are also present. Based on electric log signatures, grain size analysis, and distribution across the site, these sands are interpreted as distributary channel deposits. The clay units appear to be overbank and flood plain deposits. These interpretations are consistent with the geologic mapping performed at the site (SSAR Figures 2.5.1-4 and-5) and the interpretations by Blum and Aslan 2006 (Reference 2.4.6-16) of the Beaumont Formation that are applicable to the broader 25-mile radius site vicinity. Gravel deposits are reported in borings in the cooling basin area and in boring B-2324, which has over 30 feet (9 meters) of gravel at the top of the boring. Boring B-2324 is located on the flood plain of the Guadalupe River where gravel deposits are expected and mapped on the surface (Unit Qt on Figure 2.5.1-4).

Several criteria have been proposed for characterizing tsunami deposits and differentiating them from storm deposits. Tuttle et al. 2004 (Reference 2.4.6-13) compare deposits from the 1929 Grand Banks earthquake-induced tsunami and the 1991 "Halloween" storm. Reference 2.4.6-13 proposes that four criteria can be used to distinguish between the tsunami and storm deposits based on sedimentary characteristics, diatom content, biostratigraphic assemblages and



landscape position. These criteria are described in more detail in SSAR Subsection 2.5.1.2.5. Morton et al. 2007 (Reference 2.4.6-14) attribute the differences between tsunami and storm deposits to differences in the hydrodynamics and sediment-sorting process during transport. Shanmugam 2011 (Reference 2.4.6-15) refutes the notion that a tsunami event represents a single depositional process and contends that tsunami deposits cannot be distinguished from storm deposits using sedimentological features without considering historical information as well.

Regardless of the uncertainty in characterizing tsunami deposits and differentiating them from storm deposits, no soil deposits with the characteristics of tsunamigenic or storm surge deposition documented by Tuttle et al. 2004 or summarized by Shanmugam 2011 were encountered at VCS, nor are such deposits described by Blum and Aslan 2006 (Reference 2.4.6-16) for the site vicinity. In addition, geologic mapping and subsurface exploration do not indicate the presence of modern or paleo-geographic environments that might have preserved tsunami or storm surge deposits (SSAR 2.5.1.2.5).

2.4.6.8 References

The following are added to the reference section:

- 2.4.6-13 Tuttle, M., Ruffman, A., Anderson, T. Jeter, H., "Distinguishing Tsunami from Storm Deposits in Eastern North America: The 1929 Grand Banks Tsunami versus the 1919 Halloween Storm," Seismological Research Letters, v. 75, no. 1, p. 117-131, 2004
- 2.4.6-14 Morton, R., Gelfenbaum G., and Jaffe, B., "Physical Criteria for Distinguishing Sandy Tsunami and Storm Deposits using Modern Examples." Sedimentary Features of Tsunami Deposits-Their Origin, Recognition, and Discrimination, Tappin, D. (ed.), Sedimentary Geology, v. 200, no 3-4, (special issue) pp. 184-207, 2007.
- 2.4.6-15 Shanmugam, G., "Process-sedimentological challenges in distinguishing paleo-tsunami deposits," Natural Hazards, Springer, 2011.
- 2.4.6-16 Blum, M. D., and Aslan, A., Signatures of Climate vs. Sea-Level Change within Incised Valley-Fill Successions: Quaternary Examples from the Texas Gulf Coast, Sedimentary Geology, v. 190, p. 177-211, 2006.

SSAR Subsection 2.5.1.2.5 will be revised in a future revision to the ESPA, as indicated:

2.5.1.2.5 Site Area Geologic Hazard Evaluation

No geologic hazards have been identified within the VCS site area. No geologic units at the site are subject to dissolution. No deformation zones were encountered in the site investigation for VCS.

Volcanic activity typically is associated with subduction zones or “hot spots” in the earth’s mantle, neither of which are present within the VCS site region. Therefore, no volcanic activity is anticipated in the region.

The site area and site vicinity were investigated for evidence of prehistoric earthquakes in the form of paleoliquefaction and other anomalous geomorphic features. This investigation included aerial and ground reconnaissance within the site vicinity, analysis of stereo-paired aerial photos within the greater site area, analysis of LiDAR-derived topography within the site vicinity, and reviews of published literature. This investigation focused on identifying any anomalous geomorphic feature that may be related to strong ground shaking, including sand blows and boils, lateral spreading, and ground cracks. During this investigation, particular emphasis was placed on areas with younger, Holocene deposits (i.e., valley fill deposits along the San Antonio and Guadalupe rivers) (Figures 2.5.1-4 and 2.5.1-23), but other Pleistocene deposits were examined as well. No evidence of prehistoric earthquakes or paleoliquefaction was observed within the site area or site vicinity during this investigation.

There is no geological evidence at or within the vicinity of VCS for tsunami or storm deposits. Several criteria have been proposed for characterizing tsunami deposits and differentiating them from storm deposits. Tuttle et al. 2004 (Reference 2.5.1-271) compare deposits from the 1929 Grand Banks earthquake-induced tsunami and the 1991 “Halloween” storm and propose that four criteria can be used to distinguish between the tsunami and storm deposits. These include the following:

1. Tsunami deposits exhibit sedimentary characteristics consistent with landward transport and deposition of sediment by only a few energetic surges, under turbulent and/or laminar flow conditions, over a period of minutes to hours, whereas characteristics of storm deposits are consistent with landward transport and deposition of sediment by many more, less energetic surges, under primarily laminar flow conditions, during a period of hours to days.

2. Both tsunami and storm deposits contain mixtures of diatoms indicative of an offshore or bayward source, but tsunami deposits are more likely to contain broken valves and benthic marine diatoms.

3. Biostratigraphic assemblages of sections in which tsunami deposits occur are likely to indicate abrupt and long-lasting changes to the ecosystem coincident with tsunami inundations.

4. Tsunami deposits occur in landscape positions, including landward of tidal ponds, that are not expected for storm deposits.

Similarly, Morton et al. 2007 (Reference 2.5.1-272) attribute the differences between tsunami and storm deposits to differences in the hydrodynamics and sediment-sorting processes during transport. Morton et al. 2007 (Reference 2.5.1-272) contend that tsunami deposition results from few high-velocity, long-period waves that entrain sediment from the shore face, beach, and landward erosion zone. Tsunamis can have flow depths greater than 10 meters (33 feet), transport sediment primarily in suspension, and distribute the load over a broad region where sediment falls out of suspension when flow decelerates. In contrast, storm inundation generally is gradual and prolonged, consisting of many waves that erode beaches and dunes with no significant overland return flow until after the main flooding. Storm flow depths are commonly less than 3 meters (9.8 feet), sediment is transported primarily as bed load by traction, and the load is deposited within a zone relatively close to the beach (Reference 2.5.1-272).

Morton et al. 2007 (Reference 2.5.1-272) report that trench excavations in tsunami deposits often have a mud cap at the surface and rip-up clasts, whereas storm deposits do not. Also, the landward extent of tsunami deposits is generally considered to be greater than that of storm deposits, and tsunami deposits typically occur at higher elevations than storm deposits. This latter criteria is also noted by Tuttle et al. 2004 (Reference 2.5.1-271). Contrasting conceptual cross sections and stratigraphic columns of typical tsunami and storm deposits are shown in Figures 15 and 16 of Reference 2.5.1-272.

Dawson and Shi 2000 (Reference 2.5.1-273) cite several authors who conclude that tsunami deposits are distinctive and are frequently associated with deposition of continuous and discontinuous sediment sheets across large areas of the coastal zone and that these sheets frequently contain boulder deposits. Microfossil assemblages of diatoms and foraminifera contained within these sand sheets may provide additional information on the nature of onshore transport of sediment from deeper water; i.e., benthic foraminifera and broken diatoms.

Based on a comprehensive review of publications and postulated criteria for identifying tsunami deposits, Shanmugam 2011 (Reference 2.5.1-274) contends that alternate interpretations are viable, and distinguishing tsunami deposits from storm deposits depends on the development of criteria based on modern examples of tsunami deposits and the application of basic principles of process sedimentology.

As described in Subsections 2.5.1.2 and 2.5.4, the initial subsurface investigation at VCS included obtaining samples and data from over 150 borings drilled within and around the power block area and in the area of the cooling basin. Sixty-five cone penetration tests (CPTs), geophysical logging, and laboratory testing were also performed for the subsurface investigation. A supplemental investigation included drilling an additional 94 borings and performing 12 additional CPTs as well as geophysical logging and laboratory testing. Boring and cross section locations are shown on SSAR Figures 2.5.1-33, 2.5.4-A-1 and -A-4. Cross sections/subsurface profiles showing the unconsolidated deposits of the Beaumont Formation are presented in SSAR Figures 2.5.1-34 and -35; Figures 2.5.4-3, -5, -6, -9 and -10; Figures 2.5.4-14 through -20; and Figures 2.5.4-A-5, -6, -7, and -9 through -11. The Beaumont Formation at the site is an interbedded sequence of sands and clays with occasional gravels that extends from the ground surface to depths of about 600 feet. Subsection 2.5.1.2.3 describes site stratigraphy. In general, the sands are gray/brown/yellow, fine to medium grained silty, clayey deposits. Based on electric log signatures, grain size analysis, and distribution across the site, these sands are interpreted as distributary channel deposits. The clay units appear to be overbank and flood plain deposits. These interpretations are consistent with the geologic mapping performed at the site (SSAR Figures 2.5.1-4 and -5) and the interpretations by Blum and Aslan 2006 (Reference 2.5.1-40) of the Beaumont Formation that are applicable to the broader 25-mile radius site vicinity. Gravel deposits are reported in borings in the cooling basin area and in boring B-2324, which has over 30 feet (9 meters) of gravel at the top of the boring. Boring B-2324 is located on the flood plain of the Guadalupe River where recent alluvial gravel deposits are mapped on the surface (Unit Qt on Figure 2.5.1-4).

Regardless of the uncertainty in characterizing tsunami deposits and differentiating them from storm deposits, no soil deposits with the characteristics of tsunamigenic or storm deposition documented by Tuttle et al. 2004 (Reference 2.5.1-271) or summarized by Shanmugam 2011 (Reference 2.5.1-274) were encountered at VCS, nor are such deposits described by Blum and Aslan 2006 (Reference 2.5.1-40) for the site vicinity. In addition, geologic mapping and subsurface exploration do not indicate the presence of modern or paleo-geographic environments that might have preserved tsunami or storm surge deposits.

2.5.1.3 References

Add the following to the reference section:

- 2.5.1-271 Tuttle, M., Ruffman, A., Anderson, T. Jeter, H., "Distinguishing Tsunami from Storm Deposits in Eastern North America: The 1929 Grand Banks Tsunami versus the 1919 Halloween Storm," Seismological Research Letters, v. 75, no. 1, p. 117-131, 2004
- 2.5.1-272 Morton, R., Gelfenbaum G., and Jaffe, B., "Physical Criteria for Distinguishing Sandy Tsunami and Storm Deposits using Modern Examples." Sedimentary Features of Tsunami Deposits-Their Origin, Recognition, and Discrimination, Tappin, D. (ed.), Sedimentary Geology, v. 200, no 3-4, (special issue) pp. 184-207, 2007.
- 2.5.1-273 Dawson, A. G., and Shi, S., "Tsunami Deposits", Pure and Applied Geophysics, Vol. 157, pp. 875-897, 2000.
- 2.5.1-274 Shanmugam, G., "Process-sedimentological challenges in distinguishing paleo-tsunami deposits," Natural Hazards, Springer, 2011.

RAI 02.05.02-3(d):

Question:

In SSAR Section 2.5.2.2, the applicant discussed the EPRI-SOG model seismic source characterizations used in the PSHA for the VCS site. In accordance with 10 CFR 100.23, the staff requests the applicant provide additional information regarding its seismic source characterizations.

- d) Provide the Rondout zone 50, Law engineering 124 and Weston Geophysical Corporation 109 source zone geometries.

Response:

The Rondout source 50, Law source 124, and Weston source 109 geometries are provided below and in electronic format on the Attachment 9 CD in text file SOURCE-GEOMETRY.TXT

\$\$\$\$	ESRI	1	RONDOUT	SORCE	50	**BECDBM	000	6	050	05**	21	50
	96.97	31.78	97.36	30.56	97.85	29.77	98.62	29.40	99.51	29.40		
	101.58	29.95	102.23	30.01	102.42	29.94	102.57	29.78	102.69	29.40		
	102.85	29.25	104.56	30.66	103.82	31.51	102.75	32.68	100.87	34.41		
	99.93	34.25	96.98	33.25	95.86	33.17	96.48	32.74	96.85	32.11		
	96.97	31.78										
\$\$\$\$	ESRI	24	LAW	ENGINEERING	124	**BECDBM	\$062	5	059	00**	25	59
	104.82	36.16	104.15	35.74	103.55	35.51	102.16	35.26	100.44	35.05		
	99.41	34.69	98.64	34.42	95.75	32.73	96.36	31.76	96.68	30.19		
	97.15	29.35	98.23	28.50	99.41	28.02	100.55	27.58	101.94	27.62		
	103.31	27.88	104.61	28.60	105.16	29.24	105.32	29.51	105.57	30.12		
	105.75	31.13	105.84	33.36	105.67	34.79	105.22	35.51	104.82	36.16		
\$\$\$\$	ESRI	109	WESTON	BCK	(10)	**BECDBM	\$048	3	059	00**	26	59
	110.00	43.16	109.50	43.18	106.80	43.22	106.41	42.63	102.03	38.04		
	103.49	38.10	104.53	37.71	105.12	36.86	105.11	36.29	104.88	35.85		
	101.56	34.50	98.49	33.63	96.06	33.31	96.50	31.96	97.42	30.26		
	97.65	30.02	98.23	29.53	98.78	29.23	99.28	28.96	100.58	28.98		
	102.55	29.87	103.59	30.32	105.60	32.38	107.71	32.54	110.00	32.71		
	110.00	43.16										

Associated ESPA Revisions:

No ESPA revision is required as a result of this response.

RAI 02.05.02-4:**Question:**

In SSAR Section 2.5.2.4, the applicant discussed the probabilistic seismic hazard analysis (PSHA) conducted for the VCS site. In accordance with 10 CFR 100.23, the staff requests the applicant provide additional information regarding its PSHA.

SSAR Section 2.5.2.4.1 describes software validation using EPRI hazard calculations. The applicant indicated that the lower overall hazard calculated for each of the EPRI ESTs at the VCS site relative to the STP site is attributed to three factors, 1) ~60-mile difference in location; 2) the VCS site lying within a geographical degree cell that has lower seismicity than that of the STP site; and 3) undocumented modeling assumptions. Please explain, in detail, how these three factors combine to produce a lower hazard at the VCS site relative to the STP site.

Response:

Figure 1 shows a schematic map with the VCS and STP locations, and shows seismicity parameters in nearby degree cells. Parameters a and b are taken from EPRI-SOG files for Rondout source 51, which is the background host source for both sites. Note that low smoothing on a and constant b were specified for this source, so it depicts the spatial variation of seismicity. Also shown is parameter v_5 , which is the rate of earthquakes with $m > 5.0$ in that degree cell. Parameter a is the logarithm of the rate of earthquakes with $3.3 < m < 3.9$ in that degree cell, per equatorial square degree. Note that parameter v_5 accounts for the size of the degree cell within the source, whereas parameter a does not.

Seismic hazard from local seismicity is caused by earthquakes that occur within about 20-60 km of the site. This is illustrated in SSAR Figures 2.5.2-42 through 2.5.2-47, which show the contribution to hazard by magnitude and distance.

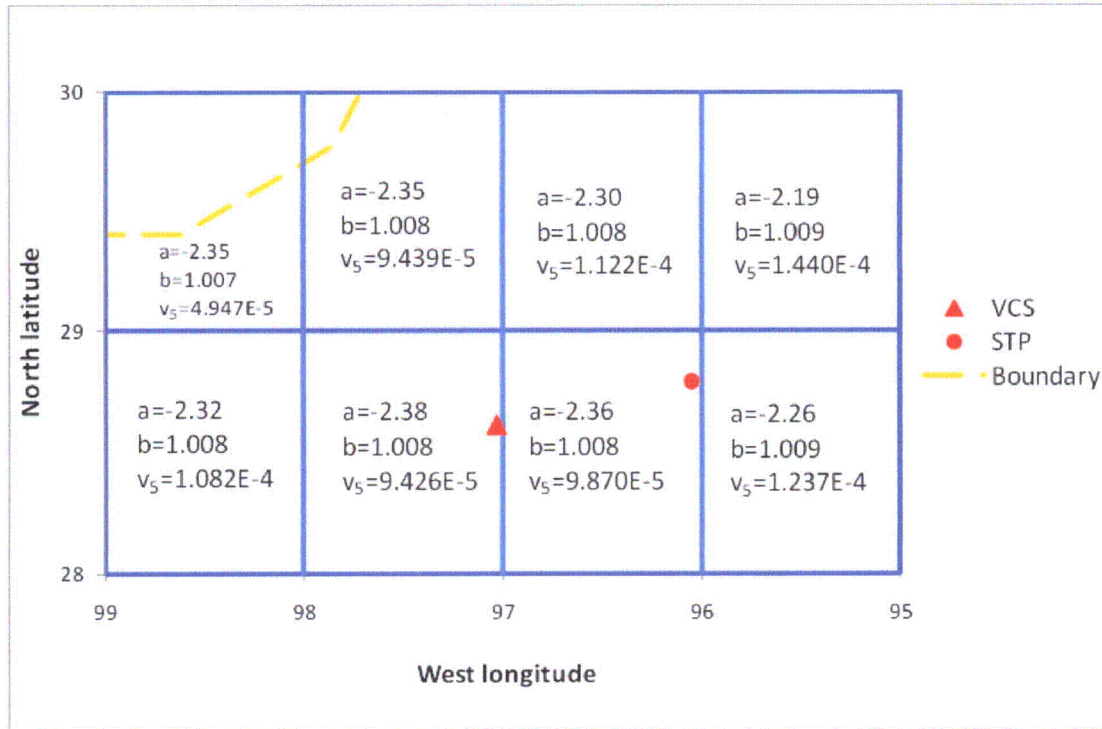


Figure 1. Schematic map showing locations of VCS and STP sites, and seismicity parameters in nearby degree cells for Rondout source 51. The dashed orange line marks the source boundary.

Figure 1 shows that the VCS site and the STP site each lie close to a whole number longitude line. A summary of the average rate parameter v_5 , for the adjacent 2 degree cells surrounding each site (the host cell and the next cell east) and for the adjacent 4 degree cells surrounding each site (the two cells just described, plus the two cells immediately north) is as follows:

Site	Average v_5 for adjacent 2 cells	Average v_5 for adjacent 4 cells
VCS	9.648E-05	9.989E-05
STP	1.112E-04	1.197E-04
VCS rate:	lower by 13%	lower by 17%

This comparison shows that seismicity in the host source (for Rondout source 51) near the VCS site is 13% to 17% lower than seismicity near the STP site, because of the location of the VCS site in a different degree cell (about 60 miles west of the STP site).

Other differences relate to undocumented assumptions in the EPRI-SOG study. For example (as discussed in the SSAR) the Woodward-Clyde team used a background

source to represent local seismicity, and this background source had an m_{\max} distribution with a value at 4.9 weighted 0.17. Under this assumption, the 15% hazard should be effectively zero, if no other sources contribute hazard. The 15% hazard reported for the STP site by EPRI-SOG indicates finite hazard, meaning that some undocumented assumption was made in the EPRI-SOG study (either regarding m_{\max} values, additional sources, or minimum hazards) that could not be replicated. These undocumented assumptions lead to a higher hazard reported in the EPRI-SOG study than the hazard calculated while attempting to replicate the EPRI-SOG results

Associated ESPA Revision:

No ESPA revision is required as a result of this response.

RAI 02.05.02-5:**Question:**

In SSAR Section 2.5.2.4.4.3, the applicant described its characterization of a new seismic source for the Rio Grande Rift (RGR). In accordance with 10 CFR 100.23, the staff requests the applicant provide additional information regarding the applicant's seismic source characterization.

- a) In SSAR Section 2.5.2.4.4.3.2, the applicant discussed simplified USGS RGR model parameters including maximum magnitudes and recurrence intervals to characterize the southern extension of the source into Mexico. Please provide the basis for applying the USGS RGR source model parameters to this southern extension. In addition, provide the basis for the applicant's simplification of the USGS RGR model parameters. For example, why did the applicant replace the maximum magnitude range from Mw 7.1 to 7.5 with a single value of Mw 7.3 for 20% of the fault population? Also, explain why the applicant replaced the otherwise lognormal-distributed RGR fault recurrence interval with discretized points. Finally, provide the line-source geometry for the hypothetical RGR southern extension.
- b) In SSAR Section 2.5.2.4.4.3.2, the applicant described its characterization of the RGR in southernmost Texas and Mexico. The applicant stated that it determined the position of the modeled RGR faults using relationships between topography, gravitational potential energy, the extent of the region of tensile stress related to the RGR, and the location of RGR-related earthquakes. SSAR Figure 2.5.2-10 shows the applicant's RGR fault characterizations overlain on a topographic map. South of "Fault 10" in SSAR Figure 2.5.2-10 and within the applicant's updated seismicity region, topographic trends continue southeastward as does the seismic activity. Please discuss the characterization of the southern extent and termination of the modeled RGR faults at Fault 10.

Response (a):

As described in SSAR Subsection 2.5.2.4.4.3, the southern extension of the Rio Grande Rift (RGR) was included in a screening study to determine whether potential RGR sources over 400 miles (640 km) from the site significantly contribute to the seismic hazard at the site. The basis for considering potential seismic sources outside of the 200-mile site region and conducting the screening study was guidance contained in NRC Regulatory Guide (RG) 1.208 that states expanded areas of investigation may be required in regions with capable tectonic sources (see RG 1.208 Section 1.2).

A hazard-informed approach was taken in conducting the screening study, where "hazard-informed" refers to the fact that the level of detail that goes into the seismic source characterization, and whether the source is included in the final probabilistic seismic hazard assessment (PSHA), depends on whether the seismic source makes a significant contribution to the site hazard. In a hazard-informed approach, initial screening studies or sensitivity analyses typically test simplified characterizations that are not thought to be unconservative to determine if a potential seismic source is likely to significantly contribute to the seismic hazard. If the simplified characterization does make a significant contribution, or is close to making a significant contribution, the characterization is refined to develop a more accurate representation of the seismic

hazard. The basis for this approach is language within RG 1.208 that suggests new information (e.g., potential seismic sources not previously considered) only needs to be included in the PSHA if they make significant contributions to the seismic hazard (see RG 1.208 Sections 2.1, 3.2, and C.3). Following this approach, the seismic source characterization for the southern extent of the RGR was developed as a “not unconservative” and simplified characterization of potential faults within the RGR as it extends into Mexico, knowing that the characterization of the southern extent of the RGR would be refined if this characterization made a significant contribution, or was close to making a significant contribution, to the site hazard.

As stated within SSAR Subsection 2.5.2.4.4.3.2, the RGR as a seismotectonic province is thought to extend into northern Mexico. However, very few Quaternary active or potentially active faults have been identified in Mexico, and those that have been identified are in northernmost Mexico near the Big Bend region of Texas (i.e., not as far south as the hypothetical faults used in the screening study) (Dickerson and Muehlberger, 1994; Keller et al., 1989). Based on the absence of identified and characterized faults, there is no data available to develop screening-level characterizations of potential faults. Therefore, assumed characteristics for hypothetical faults were used for the southern extent of the RGR. As described in SSAR Subsection 2.5.2.4.4.3.2, the locations of the hypothetical faults were taken as the closest possible approach of the RGR seismotectonic province in Mexico to the site, and the characteristics of the faults were based on the general characteristics of the RGR faults in the US. The slip rate and magnitude distributions applied to the hypothetical faults were developed by qualitatively simplifying the range of slip rates and magnitudes for the US faults characterized by the United States Geological Survey (USGS) as described in SSAR Subsection 2.5.2.4.4.3.2. The simplified characteristics were not meant to be statistically equivalent representations of the slip rates and magnitudes for the US faults; these characterizations were only meant to represent the general form of the US RGR fault characterizations. Stated differently, the slip rate and magnitude distributions used for the southern extent of the RGR were assumed distributions informed by the USGS’s characterization of RGR faults in the US. Because there is no direct data to support the assumption that any potential RGR-related faults in Mexico will have exactly the same characteristics as the faults characterized by the USGS in the US, the statistical accuracy of the hypothetical fault characterizations relative to the US fault characterizations is not material to the screening of the southern RGR extension.

Despite the lack of data available to constrain the hypothetical faults that were used in the southern extension of the RGR, the characterization of the southern extension of the RGR was considered to be conservative. The basis for this assessment is given in SSAR Subsection 2.5.2.4.4.3.2 and is that: (1) there are no known capable, potentially capable, or non-capable RGR-related faults within Mexico that are as far east as the hypothetical faults; and (2) it is unlikely that capable RGR-related faults within Mexico, if they exist, have recurrence rates or magnitudes as high as those in the US given the more pronounced topographic expression of active extension within the US compared to Mexico. In addition, if there were RGR-related faults within Mexico that are as active as those in the US, then it is more likely these faults would have been identified, and no faults have been identified beyond those in the Big Bend region.

As described in SSAR Subsection 2.5.2.4.7, the combination of all of the RGR sources used in the screening study (the US faults and the southern extent of the RGR) contribute less than 1% of the hazard for the VCS site at ground motions important for seismic design. As such, it was demonstrated that the RGR sources do not make a

significant contribution to the site hazard, do not need to be included in the site PSHA, and do not need to have more detailed characterizations.

The surface traces of the faults used in the southern extension of the RGR are provided below and in electronic format on the Attachment 10 CD in text file RGR-GEOMETRY.TXT, as longitude (°W) and latitude (°N) pairs for each fault (RGR1 to RGR10):

RGR1	RGR6
103.19 30.52	101.67 28.17
102.86 30.06	101.38 27.69
RGR2	RGR7
102.86 30.06	101.38 27.69
102.54 29.60	101.10 27.21
RGR3	RGR8
102.54 29.60	101.10 27.21
102.25 29.12	100.82 26.73
RGR4	RGR9
102.25 29.12	100.82 26.73
101.95 28.64	100.55 26.25
RGR5	RGR10
101.95 28.64	100.55 26.25
101.67 28.17	100.28 25.77

Response (b):

As described in the third paragraph of SSAR Subsection 2.5.2.4.4.3, the easternmost extent of the RGR is "...based on an estimate of the easternmost position of the large-scale lithospheric expression (elevated topography, long-wavelength gravity anomaly, elevated heat flow, tensile stress regime, region of thinned crust, and elevated mantle) and topographic expression (range-front-bounded basins) of the RGR." In this description, "topographic expression" refers to the classic basin-and-range style topography of fault-bounded basins.

In the same paragraph of SSAR Subsection 2.5.2.4.4.3, it is stated that "...the easternmost extent of each of these features roughly correlates with the elevated topography of the RGR that decays eastward to the coastal plains, so this topographic and physiographic transition to the coastal plains is used to delineate the easternmost extent of the RGR." In this sentence "topographic and physiographic transition" refers to the relative abrupt decrease in topography along which the southern extent of the RGR faults is drawn (SSAR Figure 2.5.2-10). This boundary is used to describe the easternmost extent of RGR. This boundary is not the same "topographic expression" that was earlier used to describe the basin-and-range style topography.

In the same paragraph of SSAR Subsection 2.5.2.4.4.3, it is stated that, "The southernmost possible extent of the RGR is interpreted to terminate to the south at the Sierra Madre Oriental, a Laramide fold-and-thrust belt with no evidence of extensional faulting." As indicated in this statement, the southernmost possible extent of the RGR, and thus the southernmost extent of the hypothetical faults comprising the southern extent of the RGR source, is not defined based on the "topographic and physiographic transition." Instead, the southernmost possible extent is defined based on the absence of tectonic features (e.g., extensional faulting) possibly related to the RGR. Based on this information, the placement of the southern end of "Fault 10" and the continued "topographic and physiographic transition" that extends further to the south are consistent.

Response References

Dickerson, P.W., and Muehlberger, W.R., 1994, Basins of the Big Bend segment of the Rio Grande rift, Trans-Pecos Texas, in Keller, G.R., and Cather, S.M., eds., Basins of the Rio Grande Rift: Structure, Stratigraphy, and Tectonic Setting: Boulder, CO, Geological Society of America Special Paper 291.

Keller, G.R., Hinojosa, H., Dryer, R., Aiken, L.V., and Hoffer, J.M., 1989, Preliminary investigations of the extent of the Rio Grande Rift in the northern portion of the state of Chihuahua: Geofisica Internacional, v. 28, p. 1043-1049.

Associated ESPA Revision:

No ESPA revision is required as a result of this RAI response.

RAI 02.05.02-6(a):**Question:**

In SSAR Section 2.5.2.5, the applicant describes its characterization of the seismic wave transmission characteristics for the VCS site. In accordance with 10 CFR 100.23, the staff requests the applicant provide additional information regarding the applicant's site-specific seismic wave transmission characterization.

- a) SSAR Section 2.5.2.5 describes the soil column used in soil response analysis and also referred to SSAR Section 2.5.4 for detailed soil parameters. The SSAR describes that "the base soil column for each of the two units using site-specific geotechnical and geophysical data to a depth of about 615 feet (187 m), augmented to a depth of about 8115 feet (2473 m) with deep velocity profiles taken from industry or educational resources." However, the SSAR also states that "one resource identified was oil /gas sonic well log records for deep wells drilled in the vicinity of the VCS site. Shear wave velocity data at varying depths, ranging from 117 feet (36 m) to 15860 feet (4834 m) were obtained from 6 sonic well logs located in the proximity to the VCS site." SSAR Table 2.5.4-52 lists the profile depth to 15860 ft in 200-foot intervals. Please clarify which depth was used as the bottom of the deeper soil profile for the VCS site, 8115 feet or 15860 ft.

Response:

The velocities measured in the six sonic well logs were analyzed and the results are summarized in SSAR Table 2.5.4-52 to a bottom elevation of -15,780 ft (NAVD 88), corresponding to a depth of approximately 15,860 ft. The shear wave velocity (V_s) values given in the " V_s Values for Use" column in SSAR Table 2.5.4-52 were used in the truncation analysis. This analysis shows that truncation of the soil column at 8,115 ft depth captures the frequency-dependent response of the deep soil column over all frequencies of interest, i.e., greater than 0.1 Hz. For the development of the site amplification factors, the truncated soil column from the ground surface to a depth of 8,115 ft was used.

In summary, the 15,860 ft depth was used only in the analysis to establish the truncated soil column of 8,115 ft depth. After that, all of the response analyses were based on the 8,115 ft truncated depth.

Associated ESPA Revision:

No ESPA revision is required as a result of this RAI response.

RAI 02.05.02-6(b):**Question:**

In SSAR Section 2.5.2.5, the applicant describes its characterization of the seismic wave transmission characteristics for the VCS site. In accordance with 10 CFR 100.23, the staff requests the applicant provide additional information regarding the applicant's site-specific seismic wave transmission characterization.

- b) Several tables in SSAR Section 2.5.4 list different shear wave velocity values for the site specific layers, for example, SSAR Table 2.5.4-32 and SSAR Table 2.5.4-51. Please clarify these discrepancies.

Response:

The V_s results in SSAR Table 2.5.4-32 (Geotechnical Engineering Parameters Selected for Design) are consistent with the average V_s values listed in the section titled "Power Block Area (Units 1 & 2)" of SSAR Table 2.5.4-51 (S-Wave Velocity Profile Numerical Values).

The values in the two tables are an exact match in all of the strata except for Clay 1, Clay 5 and the structural fill. The top and bottom portions of Clay 1 are separated by Sand 1. In SSAR Table 2.5.4-51, separate V_s values are given for the top and bottom portions. There is only a single value given for Clay 1 in SSAR Table 2.5.4-32, and this is the average of the top and bottom values in the SSAR Table 2.5.4-51 column labeled "Avg. V_s (ft/sec)". The same averaging was performed for Clay 5 where the top and bottom portions are separated by Sand 5.

In SSAR Table 2.5.4-32, two values are given for the V_s of the fill, and these are explained in footnote (e) of the table. The first is a representative value for the top 15 ft (700 ft/sec). In SSAR Table 2.5.4-51, three values are given for the top 15 ft of fill, i.e., 597 ft/sec for the upper fill (El. 95 ft to El. 90 ft), 708 ft/sec for the middle fill (El. 90 ft to El. 85 ft), and 783 ft/sec for the lower fill (El. 85 ft to El. 80 ft). The average of these three values (696 ft/sec) is rounded to give the 700 ft/sec in Table 2.5.4-32.

The second fill V_s value in Table 2.5.4-32 (1,000 ft/sec) is the approximate average V_s from 15 ft depth (El. 80 ft) to the bottom of the deepest excavation at 110 ft depth (El. -15 ft). This depth range for fill is not covered in Table 2.5.4-51.

Associated ESPA Revisions:

SSAR Table 2.5.4-51 will be revised as shown in the attached page in a future revision to the ESPA.

Table 2.5.4-51 (Sheet 2 of 3)
S-Wave Velocity Profile Numerical Values; Upper Approximately
600 Feet of Site Soils (Power Block Area)

Stratum	Top El. (feet) ^(a)	Base El. (feet) ^(a)	Max. V _s (ft/sec)	Min. V _s (ft/sec)	Median V _s (ft/sec)	Avg. V _s (ft/sec)	Std. Dev. (ft/sec)	No. of Tests
Power Block Area (Unit 2) (continued)								
Clay 5 (Btm)	-66.0	-79.0	1740	790	1110	1119	175	31
Sand 6	-79.0	-128.5	3400	490	1365	1421	401	128
Clay 7	—	—	—	—	—	—	—	—
Sand 8	-128.5	-204.0	3000	1140	1750	1737	347	82
Clay 9	-204.0	-248.0	1750	990	1250	1250	149	50
Sand 10	-248.0	-289.0	2020	1270	1660	1645	192	51
Clay 11	-289.0	-323.0	1410	910	1100	1102	113	36
Sand 12	-323.0	-326.0	2190	1610	1860	1866	147	14
Clay 13	-326.0	-422.0	2270	1050	1280	1312	184	46
Sand 14	-422.0	-468.5	2400	1370	1870	1885	196	29
Clay 15	-468.5	-481.0	1560	1360	1410	1436	88	7
Sand 16	-481.0	-499.0	1980	1540	1750	1765	125	11
Clay 17	-499.0	-515.0	2120	1950	2060	2050	63	10
Sand 18	-515.0	-520.0	2040	1940	2000	1993	50	3
Power Block Area (Units 1 & 2)								
Fill (Upper)	95.0	90.0	—	—	—	597	—	—
Fill (Middle)	90.0	85.0	—	—	—	708	—	—
Fill (Lower)	87.0 85.0	80.0	—	—	—	783	—	—
Clay 1 (Top)	80.0	51.5	1160	167	670	671	185	142
Sand 1	51.5	43.0	1350	738	1079	1080	154	32
Clay 1 (Btm)	43.0	30.5	1560	470	835	899	246	108
Sand 2	30.5	18.5	1470	570	1040	1060	198	55
Clay 3	18.5	-5.5	1670	490	990	992	243	175
Sand 4	-5.5	-32.0	5380	687	1460	1603	737	128
Clay 5 (Top)	-32.0	-51.0	2870	700	1060	1135	318	95
Sand 5	-51.0	-64.0	2490	870	1375	1376	316	34
Clay 5 (Btm)	-64.0	-73.5	1740	790	1110	1137	213	67
Sand 6	-73.5	-127.5	3400	490	1390	1479	405	265
Clay 7	-127.5	-172.5	2010	800	1480	1445	339	33
Sand 8	-172.5	-205.5	3000	980	1630	1655	353	140
Clay 9	-205.5	-250.0	1750	990	1260	1252	132	112
Sand 10	-250.0	-278.5	2220	1160	1660	1652	221	74
Clay 11	-278.5	-325.5	1750	820	1130	1146	169	95
Sand 12	-325.5	-346.0	2190	1580	1840	1846	138	25
Clay 13	-346.0	-421.5	2310	1020	1310	1361	231	92
Sand 14	-421.5	-461.5	2400	1370	1840	1842	180	49
Clay 15	-461.5	-473.0	1800	1100	1445	1479	183	14
Sand 16	-473.0	-489.5	1980	1540	1745	1788	118	20

RAI 02.05.02-9:**Question:**

In SSAR Section 2.5.2.4, the applicant discussed the probabilistic seismic hazard analysis (PSHA) conducted for the VCS site. In accordance with 10 CFR 100.23, the staff requests the applicant provide additional information regarding its PSHA. SSAR Section 2.5.2.4.7 describes the applicant's incorporation of site-specific hazard at the VCS site.

- a) SSAR Figure 2.5.2-18 shows the 10 Hz mean rock hazard curves for the New Madrid seismic zone (NM) only and the EPRI-SOG+NM. SSAR Figure 2.5.2-24 shows the mean rock seismic hazard curves by source for each EPRI EST source and the New Madrid source. Please explain why the total hazard [EPRI-SOG+NM curve] in SSAR Figure 2.5.2-18 does not appear to reflect the sum of the individual hazard curves in SSAR Figure 2.5.2-24.
- b) In SSAR Figure 2.5.2-38, the mean hazard curve exceeds the 95 percentile hazard curve at 0.09 g and above. Please explain this result.

Response (a):

SSAR Figure 2.5.2-24 shows 10 Hz seismic hazard curves by seismic source for the six EPRI-SOG teams and for the New Madrid (NM) source. In this figure a weight of 1.0 has been used for all sources, to allow comparison between hazard from the EPRI-SOG team sources and the NM source. To calculate total hazard as shown in SSAR Figure 2.5.2-18, the EPRI-SOG team sources must be weighted by 1/6 each because these are alternative interpretations that were weighted 1/6 each in the EPRI-SOG study, prior to summing the hazard.

Response (b):

In SSAR Figure 2.5.2-38 the mean hazard curve exceeds the 95 percentile hazard curve at ground motions of 0.09g and above because the percentile hazard curves include epistemic uncertainty in ground motion equations, and there is a large range of hazard over this epistemic uncertainty. This range is illustrated in Figure 1, which shows contribution by ground motion equation for the NM source (this source contributes virtually all seismic hazard for low spectral frequencies, as shown in SSAR Figure 2.5.2-19 for 1 Hz spectral acceleration). In Figure 1, the ground motion equation labeled "F9" is the highest curve and this dominates the calculation of the mean hazard. As an example, the following table shows an approximate, illustrative calculation of mean hazard for 0.5 Hz spectral acceleration at 0.09g (taken from the curves illustrated in Figure 1), using only the highest 3 hazard curves in that figure:

Ground motion equation	Weight	Approximate hazard at 0.09g	Weighted hazard (weight x approx. haz.)
F9	0.036	4×10^{-4}	1.4×10^{-5}
F8	0.123	7×10^{-6}	8.6×10^{-7}
FB	0.040	3×10^{-6}	1.2×10^{-7}
Total mean hazard	—	—	1.5×10^{-5}

The last row in the above table sums the weighted hazards from the highest 3 hazard curves, and shows that the approximate total mean hazard is 1.5×10^{-5} (which agrees with the “mean” curve in SSAR Figure 2.5.2-38 at 0.09g), and that the dominant contribution to this hazard comes from the highest ground motion equation “F9”. Since only one hazard curve lies above this hazard at 0.09g (ground motion equation “F9” with a weight of 0.036), it is reasonable that the total mean hazard lies at about the 95 percentile of epistemic uncertainty in hazard at 0.09g.

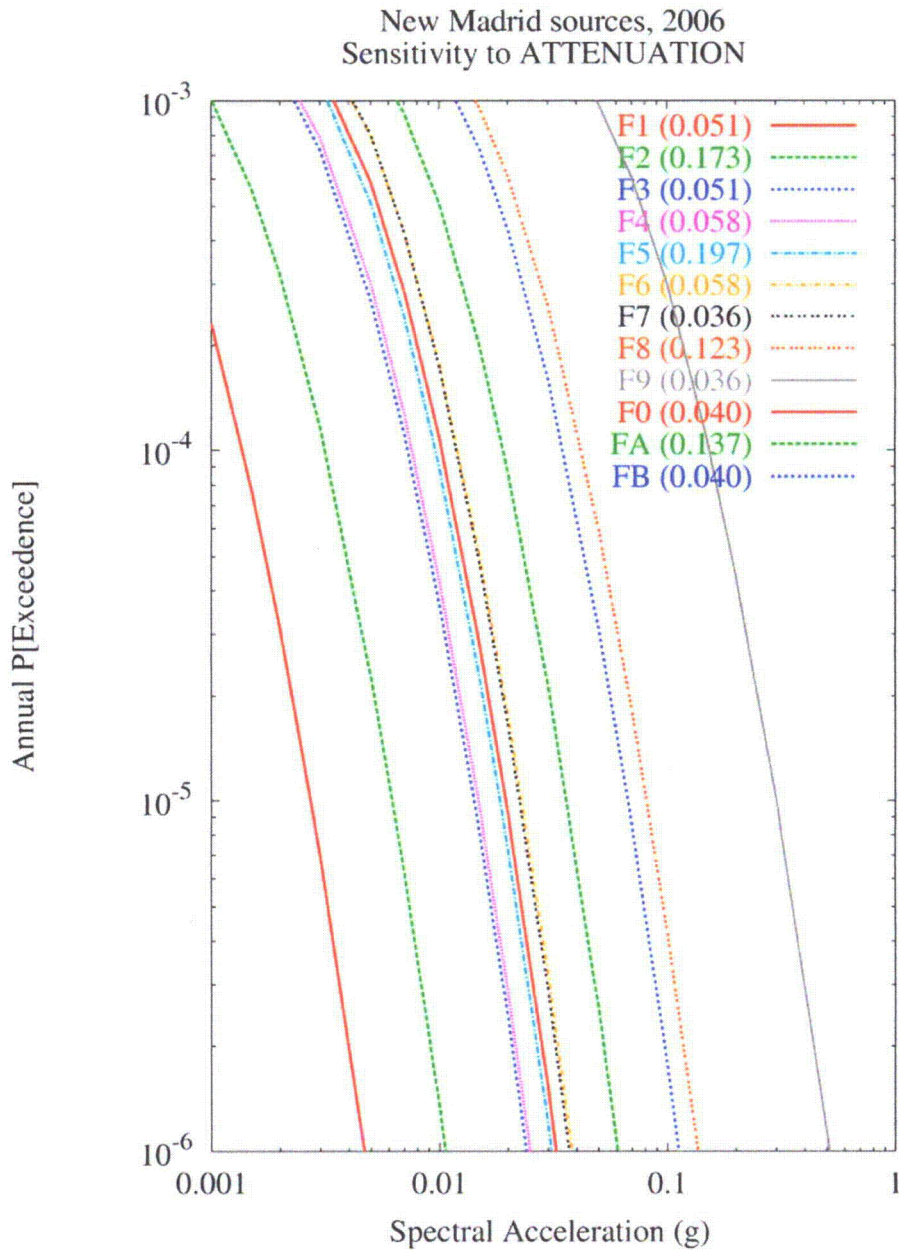


Figure 1. Sensitivity of 0.5 Hz rock hazard to ground motion equation for New Madrid faults.

Associated ESPA Revision:

No ESPA revision is required as a result of this RAI response.

ATTACHMENT 8

SUMMARY OF REGULATORY COMMITMENTS

(Exelon Letter to USNRC, NP-11-0020, dated May 23, 2011)

The following table identifies commitments made in this document. (Any other actions discussed in the submittal represent intended or planned actions. They are described to the NRC for the NRC's information and are not regulatory commitments.)

COMMITMENT	COMMITTED DATE	COMMITMENT TYPE	
		ONE-TIME ACTION (Yes/No)	Programmatic (Yes/No)
<p>Exelon will revise the VCS ESPA SSAR Sections 2.4.6 and 2.5.1 to incorporate the changes shown in the enclosed response to the following NRC RAI:</p> <p>02.04.06-2 (Attachment 1)</p>	<p>Revision 1 of the ESPA SSAR and ER planned for no later than March 31, 2012</p>	<p>Yes</p>	<p>No</p>
<p>Exelon will revise the VCS ESPA SSAR Section 2.5.4 to incorporate the changes shown in the enclosed response to the following NRC RAI:</p> <p>02.05.02-6(b) (Attachment 6)</p>	<p>Revision 1 of the ESPA SSAR and ER planned for no later than March 31, 2012</p>	<p>Yes</p>	<p>No</p>

ATTACHMENT 9

CD-R labeled:

RAI 02.05.02-3(d) SOURCE-GEOMETRY.TXT

(Two copies)

ATTACHMENT 10

CD-R labeled:

RAI 02.05.02-5 RGR-GEOMETRY.TXT

(Two copies)